

1

2 **Unstable Surface Modes in Finite Chain Computations:** 3 **Deficiency of Reflection Coefficient Approach**

4 Shaoqiang Tang* and Ming Fang

5 *Center for Applied Physics and Technology, and LTCS, College of Engineering,*
6 *Peking University, Beijing 100871, China.*

7 Received 9 April 2009; Accepted (in revised version) 5 October 2009

8 Available online xxx

10

Abstract. In this paper, we investigate the stability for a finite harmonic lattice under a certain class of boundary conditions. A rigorous eigenvalue study clarifies that the invalidity of Fourier modes as the basis results in the deficiency of standard reflection coefficient approach for stability analysis. In a certain parameter range, unstable surface modes exist in the form of exponential decay in space, and exponential growth in time. An approximate eigen-polynomial is proposed to ease the stability analysis. Moreover, the eigenvalues with small positive real part quantitatively explain the long time instability in wave propagation computations. Numerical results verify the analysis.

11 **PACS:** 43.20.+g, 83.10.Rs, 63.20.D-

12 **Key words:** Unstable surface mode, reflection coefficient, finite chain.

13

14 **1 Introduction**

15 Interfaces/surfaces are of fundamental importance in materials science and engineering.
16 Substantial understanding of the physics has been obtained through studies on wave
17 propagations across an interface/surface. Generally speaking, the two materials across
18 an interface/surface yield different dispersion relations. Continuity of the wave function
19 requires a certain combination of waves with different propagation directions. Wave fea-
20 tures are then usually characterized by the reflection and transmission coefficients. In
21 the mean time, interfaces/surfaces also play an important role in numerical computa-
22 tions. For instance, in a multi-scale computation that couples atomistic dynamics and
23 continuum deformation, atomistic fluctuations need to be damped out through suitable
24 boundary conditions. As it is virtually impossible to cleanly transmit all fluctuations,
25 the reflected part enters back and cause spurious wave interactions inside the atomistic

*Corresponding author. *Email address:* maotang@pku.edu.cn (S. Tang)

26 domain. Hence a key ingredient for a multi-scale algorithm is the design of interfacial
 27 conditions for reflection reduction. In the literature, numerical absorption treatments
 28 have been proposed, including a perfect matched layer, or a time history kernel convolu-
 29 tion, or a velocity interfacial condition, etc [1,5,20,23–25]. Most of these methods adopt a
 30 sinusoidal Fourier mode viewpoint, and are validated or analyzed through the resulted
 31 reflection coefficients. A dynamic atomistic-continuum algorithm is even designed by
 32 minimizing the reflection coefficient within a certain range of wave-numbers [6]. In ad-
 33 dition, for continuous wave propagation in an unbounded domain, one assigns a finite
 34 computing domain. Numerical boundary conditions are then also analyzed and opti-
 35 mized through the reflection coefficient approach [3,7,10,12,13,17,27]. We remark that
 36 rigorous analysis had also been performed for continuous wave equations by Kreiss and
 37 others [8,14], and for discrete schemes by Halpern, Li, and others [9,15].

38 In this paper, we study carefully the validity of the reflection coefficient approach for
 39 wave propagation applications. As is known for a long time, the Fourier modes do not
 40 completely or accurately describe the wave features for finite lattice chains. We quanti-
 41 tatively demonstrate, with a velocity interfacial condition, that this invalidity results in
 42 the deficiency of the reflection coefficient approach and incorrect stability results. We
 43 observe unstable surface modes in a parameter range where the reflection coefficient ap-
 44 proach claims to be stable. An approximate eigen-polynomial is proposed, which has
 45 a much lower order than the full problem. This may greatly ease a rigorous stability
 46 analysis. The eigen modes are classified into unstable surface modes, absorption modes,
 47 and vibration/propagation modes. Our results reveal the complexity of wave propaga-
 48 tions in multiple media, and urges for substantiating numerical analysis for multi-scale
 49 computations. We remark that the finite size effects may lead to possible discoveries for
 50 micro-/nano-materials, similar to those for electronic states in a finite crystal [22].

51 The rest of the paper is arranged as follows. We describe the governing equations
 52 and the reflection coefficient approach for a finite chain in Section 2. Then a full eigen-
 53 problem study is performed in Section 3. Numerical tests are also presented. In Section
 54 4, we discuss long time instability, which is a subtle issue in numerical simulations and
 55 quantitatively explained by the current eigen-problem results. We make some concluding
 56 remarks in Section 5.

57 2 Reflection coefficient

We consider a harmonic lattice consisting $(N+2)$ atoms. The n -th atom deviates from its
 equilibrium by a displacement $u_n(t)$, and a velocity $v_n(t) = \dot{u}_n(t)$. We impose the same
 type of boundary conditions at both ends. The governing system is as follows.

$$\dot{u}_0 = \alpha u_0 + \beta u_1, \quad (2.1a)$$

$$\dot{u}_n = v_n, \quad n = 1, \dots, N, \quad (2.1b)$$

$$\dot{v}_n = u_{n-1} - 2u_n + u_{n+1}, \quad n = 1, \dots, N, \quad (2.1c)$$

$$\dot{u}_{N+1} = \alpha u_{N+1} + \beta u_N. \quad (2.1d)$$

58 Here α and β are constants. In a reflection coefficient approach, one actually considers
59 a semi-infinite chain instead, e.g., $n = 0, 1, 2, \dots$. A monochromatic wave is decomposed
60 into a transmission component and a reflection component.

$$u_n(t) = e^{i(\omega t - kn)} + R e^{i(\omega t + kn)}. \quad (2.2)$$

61 From the Newton equations of the inner atoms, the frequency ω and the wave number
62 $0 \leq k \leq \pi$ are related by the dispersion relation $\omega = 2\sin(k/2)$. Substituting this into the
63 boundary condition, we obtain the reflection coefficient

$$R(k) = -\frac{(\alpha + \beta \cos k) + i(\beta \sin k - 2\sin(k/2))}{(\alpha + \beta \cos k) + i(\beta \sin k + 2\sin(k/2))}. \quad (2.3)$$

64 From this expression, it is obvious that $|R| < 1$ for $\beta > 0$, and $|R| > 1$ for $\beta < 0$. For a
65 finite chain, it is widely conceived that $|R| < 1$ indicates energy decay and hence stability.
66 A possible interpretation is as follows. When a localized one-way wave package reaches
67 at the boundary, each Fourier mode is partially transmitted. Because $|R| < 1$, the reflec-
68 tion part has a smaller amplitude than the incident wave, and alternates the propagation
69 direction. By virtue of the Parseval's relation, the whole reflection wave package has a
70 smaller energy. The energy repeatedly decreases when the wave package reaches at ei-
71 ther end. By a similar argument, instability is expected if $|R(k)| > 1$ for a certain range of
72 k .

73 This interpretation assumes the Fourier mode decomposition. Later we shall com-
74 pute the eigen-modes, which turn out to be not the Fourier modes for the finite chain
75 with generic boundary conditions. In particular, because instability emerges in the form
76 of non-Fourier modes, the reflection coefficient approach may not be suitable for the sta-
77 bility analysis.

78 In solid state physics, an infinite periodic lattice is usually assumed. Though it is
79 known for long time that a real finite lattice does not possess the Fourier eigen modes,
80 the deviation is not precisely identified, and is believed to be negligible for a lattice
81 big enough. On the other hand, for a multiscale computation, the finite lattice consid-
82 ered here corresponds to the atomistic subdomain, where fine scale calculations are per-
83 formed. A surrounding infinite periodic lattice is assumed to be at equilibrium initially. If
84 an exact/transparent interfacial condition is posed, e.g., in the time history convolution
85 form, the Fourier modes still serve as the basis provided that the atomistic subdomain
86 has the same lattice structure. However, this does not hold when either a non-exact in-
87 terfacial condition is adopted due to time cut-off or discretization error, or the atomistic
88 subdomain has a different lattice structure. For such cases, the eigen modes are not in the
89 form of Fourier modes in the atomistic subdomain, even if they are so in the surrounding
90 lattice. Moreover, the atomistic subdomain together with the interfacial condition forms
91 a closed system. With the bridging scale technique, for instance, this closed system de-
92 scribes the fluctuation part of the motion in the atomistic subdomain. For both theoretical

93 and numerical error analysis of interfacial conditions, one actually considers the reflection of the atomistic subdomain. Therefore, a substantial understanding of the dynamic system (2.1a)-(2.1d) is crucial for both the physics and the multiscale computations.

96 3 Eigenvalue study for finite chain

97 We perform a complete eigenvalue study to substantiate the understanding on wave properties of the finite chain.

99 3.1 Eigenvalue problem

100 Since the governing system is linear, we may find the eigenvalues and eigenvectors for the coefficient matrix on the right hand side. The motion of the lattice is then explicitly expressed as a superposition of these eigen-modes.

In addition to the standard matrix approach, an eigen-mode may also be obtained as a solution in the form of $u_n(t) = \tilde{u}_n e^{\lambda t}$ and $v_n(t) = \lambda \tilde{u}_n e^{\lambda t}$. The time-independent variables $\{\tilde{u}_n\}$ solve

$$\lambda \tilde{u}_0 = \alpha \tilde{u}_0 + \beta \tilde{u}_1, \quad (3.1a)$$

$$\lambda^2 \tilde{u}_n = \tilde{u}_{n-1} - 2\tilde{u}_n + \tilde{u}_{n+1}, \quad n = 1, \dots, N, \quad (3.1b)$$

$$\lambda \tilde{u}_{N+1} = \alpha \tilde{u}_{N+1} + \beta \tilde{u}_N. \quad (3.1c)$$

103 From (3.1b), we have a general expression for $\{\tilde{u}_n\}$ as follows:

$$\tilde{u}_n = A q_+^n + B q_-^n. \quad (3.2)$$

Here

$$q_{\pm} = [\lambda^2 + 2 \pm \lambda \sqrt{\lambda^2 + 4}] / 2 \neq 0$$

104 are the two roots to

$$q^2 - (\lambda^2 + 2)q + 1 = 0. \quad (3.3)$$

105 Substituting this into (3.1a) and (3.1c), we find that the coefficients A and B satisfy

$$\begin{bmatrix} \lambda - \alpha - \beta q_+ & \lambda - \alpha - \beta q_- \\ (\lambda - \alpha) q_+^{N+1} - \beta q_+^N & (\lambda - \alpha) q_-^{N+1} - \beta q_-^N \end{bmatrix} \begin{bmatrix} A \\ B \end{bmatrix} = 0. \quad (3.4)$$

106 Nontrivial solutions A and B exist only when the coefficient matrix is singular. Due to $q_- q_+ = 1$, the condition amounts to

$$-q_-^{N+1} \left\{ [(\lambda - \alpha) q_+ - \beta] q_+^N + [\lambda - \alpha - \beta q_+] \right\} \left\{ [(\lambda - \alpha) q_+ - \beta] q_+^N - [\lambda - \alpha - \beta q_+] \right\} = 0. \quad (3.5)$$

108 The eigenvalues are therefore roots to the eigen-polynomials

$$V_N^{\pm}(\lambda) = q_+^N [(\lambda - \alpha) q_+ - \beta] \pm [\lambda - \alpha - \beta q_+] = 0. \quad (3.6)$$

109 In particular, for an eigenvalue λ that is a root to $V_N^+(\lambda)$, it holds that $\lambda - \alpha = \beta(q_+^N +$
 110 $q_+)/ (q_+^{N+1} + 1)$. We take

$$A = (\lambda - \alpha - \beta q_-) \frac{q_+^{N+1} + 1}{\beta(q_+^{N+1} - q_+^{N-1})}, \quad B = [-(\lambda - \alpha) + \beta q_+] \frac{q_+^{N+1} + 1}{\beta(q_+^{N+1} - q_+^{N-1})}. \quad (3.7)$$

111 After some algebra, we compute the eigenvector as

$$\tilde{u}_n = q_+^{-n+1} + q_+^{n-N}, \quad n = 0, \dots, N+1. \quad (3.8)$$

112 Because $\tilde{u}_{N+1-n} = \tilde{u}_n$, the eigenvector is symmetric.

113 Next, we check the eigenvalues and eigenvectors in more details. Let $q = \rho e^{i\theta}$. We may
 114 rewrite equation (3.3) as

$$\lambda = \pm(q^{1/2} - q^{-1/2}) = \pm \left[(\sqrt{\rho} - \frac{1}{\sqrt{\rho}}) \cos \frac{\theta}{2} + i(\sqrt{\rho} + \frac{1}{\sqrt{\rho}}) \sin \frac{\theta}{2} \right]. \quad (3.9)$$

Therefore, for an eigenvalue λ with $|\operatorname{Re}\lambda|$ not small, the corresponding $|q_+|$ is away from 1 by an amount not small. There are two consequences for such an eigenvalue. First, the components of the corresponding eigenvector are negligible for n not close to 0 or $(N+1)$, compared with the components

$$\tilde{u}_0 = \tilde{u}_{N+1} = q_+ + q_+^{-N}.$$

115 In addition, the components for n close to 0 or $(N+1)$ decay on the order of q_+^{-n+1} or
 116 q_+^{n-N} . The eigen-mode is therefore a kind of surface mode, decaying exponentially in
 117 space away from the surface. Secondly, because either $|q_+^N| \gg 1$ or $|q_+^N| \ll 1$ in (3.6) for a
 118 chain long enough, the eigenvalue approximately solves either

$$(\lambda - \alpha)q_+ - \beta = 0, \quad (3.10)$$

119 or

$$(\lambda - \alpha) - \beta q_+ = 0. \quad (3.11)$$

120 In both cases, λ is approximately a root to the cubic polynomial

$$\beta\lambda^3 - (1 + \alpha\beta)\lambda^2 + 2(\alpha + \beta)\lambda - (\alpha + \beta)^2 = 0, \quad (3.12)$$

121 subject to the constraint

$$|\lambda - \alpha| < |\beta|. \quad (3.13)$$

122 This serves as a simplified eigen-polynomial for stability analysis. Compared with (3.6),
 123 it has a much lower order.

124 Similarly, for an eigenvalue λ that is a root to $V_N^-(\lambda)$, it holds that $\lambda - \alpha = \beta(q_+^N -$
 125 $q_+)/ (q_+^{N+1} - 1)$. The eigenvector is found to be

$$\tilde{u}_n = q_+^{-n+1} - q_+^{n-N}, \quad n = 0, \dots, N+1. \quad (3.14)$$

126 It is antisymmetric with respect to the space, namely, $\tilde{u}_{N+1-n} = -\tilde{u}_n$. When $|\operatorname{Re}\lambda|$ is not
 127 small, an eigen-mode is a surface mode, and λ approximately solves (3.12). Moreover,
 128 after some algebraic calculations, we find that the only situation for $V_N^+(\lambda)$ and $V_N^-(\lambda)$ to
 129 possess a common root is $\lambda = 0$ under the condition $\alpha + \beta = 0$.

130 3.2 Unstable surface modes

In this subsection, we seek for a positive eigenvalue λ . Noticing that when $\lambda \geq 0$, we have $q_+ \geq \lambda^2 + 1$. Hence as $\lambda \rightarrow +\infty$, it holds that

$$V_N^\pm(\lambda) \sim (\lambda - \alpha)q_+^{N+1} \rightarrow +\infty.$$

On the other hand, we observe that $q_+ = 1$ at $\lambda = 0$. It gives $V_N^+(0) = -2(\alpha + \beta)$, and $V_N^-(0) = 0$. We further compute $\frac{dq_+}{d\lambda}(0) = 1$, and

$$\begin{aligned} \frac{dV_N^-(0)}{d\lambda} &= \left\{ q_+^{N+1} - 1 + [(\lambda - \alpha)(N+1)q_+^N - \beta N q_+^{N-1} + \beta] \frac{dq_+}{d\lambda} \right\}_{\lambda=0} \\ &= -[(\alpha + \beta)N + (\alpha - \beta)]. \end{aligned} \quad (3.15)$$

131 Similarly, we compute for $\lambda = \alpha$.

$$V_N^+(\alpha) = -\beta q_+(q_+^{N-1} + 1), \quad V_N^-(\alpha) = -\beta q_+(q_+^{N-1} - 1). \quad (3.16)$$

132 By the intermediate value theorem, we find that a positive eigenvalue λ_+ exists for
133 $V_N^+(\lambda_+) = 0$ if $\alpha + \beta > 0$. The eigenvalue $\lambda_+ > \alpha$ if both α and β are positive. There also
134 exists another positive eigenvalue $\lambda_- > 0$ for $V_N^-(\lambda_-) = 0$, if $\alpha + (N-1)\beta / (N+1) > 0$. The
135 eigenvalue $\lambda_- > \alpha$ if both α and β are positive.

136 For a positive eigenvalue λ , the corresponding $q_+(\lambda) \geq \lambda^2 + 1$. As discussed in the
137 previous section, it is a root to (3.12). In particular, the difference between λ_- and λ_+
138 is negligible when N is big. Furthermore, the corresponding eigen-modes are surface
139 modes. We remark that the surface mode is purely a standing wave without propagation,
140 which grows exponentially in time [2, 4, 18, 21].

We further remark that when $\alpha + \beta = 0$, the total energy

$$E(t) = \frac{1}{2} \sum_{n=1}^N v_n(t)^2 + \frac{1}{2} \sum_{n=0}^N (u_{n+1}(t) - u_n(t))^2$$

141 decreases if $\alpha < 0$, increases if $\alpha > 0$, and conserves if $\alpha = 0$. The last case corresponds to a
142 fixed boundary.

143 3.3 Numerical tests

144 We illustrate the previous analysis by numerical tests. In particular, we take $\alpha = -1, \beta = 2$.
145 The modulus of the reflection coefficient is depicted in Fig. 1. It is less than 1 except at
146 $k = 0$ and π .

147 For a relatively short lattice with $N = 20$, the 42 eigenvalues are displayed in Fig. 2.
148 There are three types of eigenvalues. First, there are a pair of positive real eigenvalues,
149 giving rise to the unstable surface modes. Even in such a short chain, they are very
150 close. The second type includes two pairs of eigenvalues with real parts about -0.438.

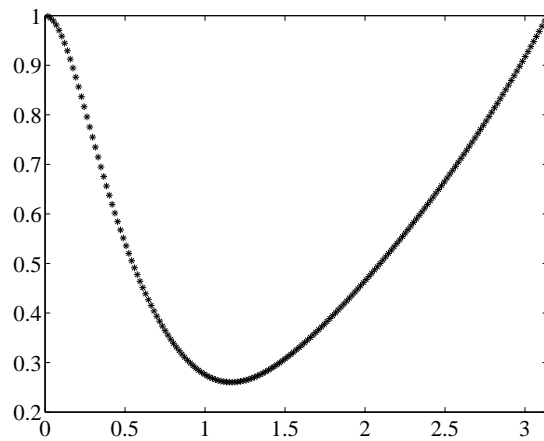


Figure 1: Reflection coefficient for $\alpha = -1, \beta = 2$: the horizontal axis denotes the wave number k , and the vertical axis denotes the reflection coefficient $|R|$.

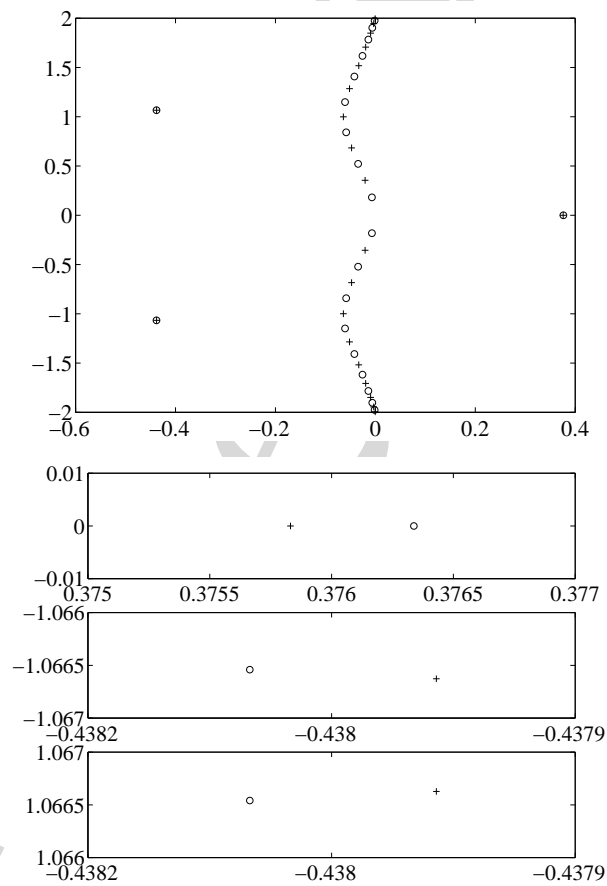


Figure 2: Eigenvalues for $\alpha = -1, \beta = 2, N = 20$ in the complex plane. The last three subplots are zoom-in view of the 3 pairs of eigenvalues. '+' : roots to $V_N^+(\lambda)$; 'o': roots to $V_N^-(\lambda)$.

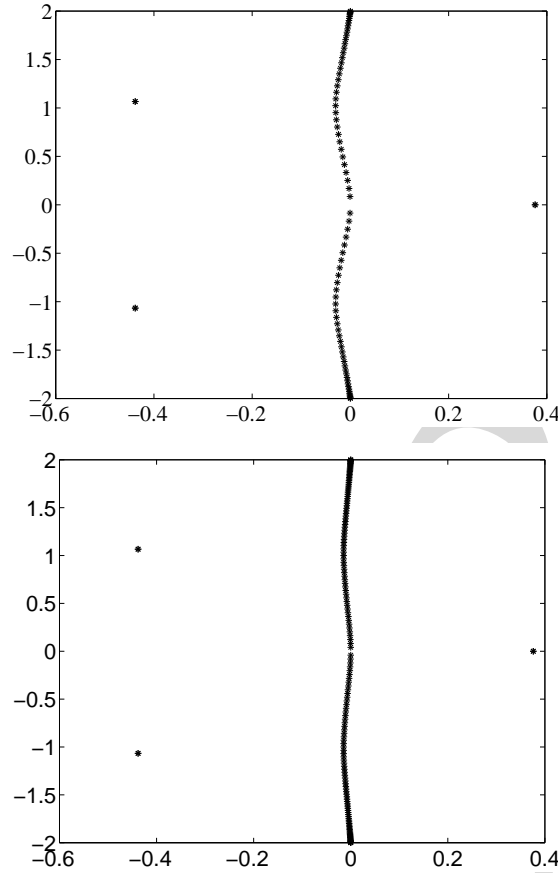


Figure 3: Eigenvalues for $\alpha = -1, \beta = 2$ in the complex plane: top $N = 40$, bottom $N = 80$.

151 The corresponding eigen-modes are effectively absorbed. We refer to these modes as the
 152 absorption modes. The subplots show the details for these eigenvalues. The above three
 153 pairs of eigenvalues are approximately the roots to (3.12). The third type, located near
 154 the imaginary axis, includes all other eigenvalues. Their real parts are between -0.06398
 155 and -0.00037 . The corresponding eigen-modes are stable, and are damped out very
 156 slowly. They are referred as vibration/propagation modes. Checking the symmetry for
 157 eigenvectors, we may detect whether an eigenvalue is a root to $V_N^+(\lambda)$ or $V_N^-(\lambda)$.

158 For a longer chain, the first two types of eigenvalues remain unchanged, whereas the
 159 third type of eigenvalues get closer to the imaginary axis. See Fig. 3. For instance, the
 160 real parts of these eigenvalues are between -0.0301 and -4.716×10^{-5} for $N = 40$; and
 161 between -0.0146 and -5.914×10^{-6} for $N = 80$. More detailed numerical computations
 162 show that the minimal real part goes on the order of $\mathcal{O}(N^{-1})$.

163 Some eigen-modes are displayed in Fig. 4 for a chain with 42 atoms. The two unsta-
 164 ble surface modes are shown in the first two subplots. They are real. The exponential
 165 decay away from the surface is evident. In contrast, the absorption modes in the next

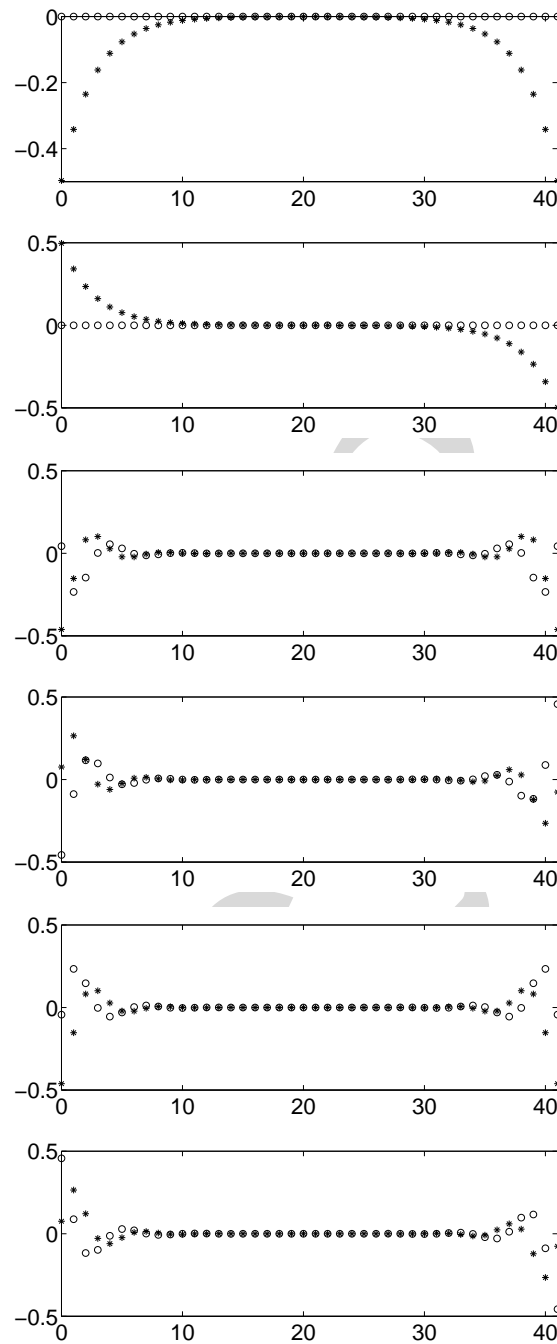


Figure 4: Eigen-modes for a chain with $N=40$: '*' represents the real part, and 'o' represents the imaginary part. Subplots from top to bottom: eigen-mode for eigenvalue 0.376086 of $V_N^+(\lambda)$; eigen-mode for eigenvalue 0.376086 of $V_N^-(\lambda)$; eigen-mode for eigenvalue $-0.43804+1.06658i$ of $V_N^+(\lambda)$; eigen-mode for eigenvalue $-0.43804+1.06658i$ of $V_N^-(\lambda)$; eigen-mode for eigenvalue $-0.43804-1.06658i$ of $V_N^+(\lambda)$; eigen-mode for eigenvalue $-0.43804-1.06658i$ of $V_N^-(\lambda)$.

166 four subplots are complex, and oscillations present near the boundaries. As in both the
 167 unstable modes and the absorption modes the inner atoms are essentially motionless,
 168 the instability and absorption are observable only around the boundary. Moreover, the
 169 third and fifth subplots are complex conjugates. So for the fourth and sixth subplots. The
 170 numerical results verify the previous analysis.

171 Comparing with the stability condition $\beta > 0$ from the reflection coefficient analysis,
 172 we observe that instability actually occurs when $\alpha + \beta > 0$. The reflection coefficient ap-
 173 proach gives irrelevant stability statement for the finite chain. This is due to the fact that
 174 the Fourier modes in the form of $\tilde{u}_n = e^{ikn}$ do not comply with the surface modes. Instead
 175 of sinusoidal forms, the surface modes have exponential decay profiles. The absorption
 176 modes do not have sinusoidal profiles either. Because the basis or general solution to the
 177 governing system (2.1a)-(2.1d) differs from the Fourier modes, the reflection coefficient
 178 approach naturally does not yield a correct stability result. Though the invalidity of the
 179 Fourier modes has been known for a long time, our analysis quantitatively clarify this
 180 point and its consequences.

181 4 Long time instability

We consider a special case when $0 < \alpha + \beta \equiv \delta \ll 1$. In addition, we assume that $\delta = o(1/N)$.
 We expect a very small positive eigenvalue λ corresponding to $V_N^+(\lambda) = 0$. Taking a
 leading order approximation $\lambda = a\delta + o(\delta)$, we easily find that $q_+ = 1 + a\delta + o(\delta)$, and $q_+^N =$
 $1 + Na\delta + o(\delta)$. Using repeatedly $\delta = \alpha + \beta$, we compute

$$\begin{aligned} V_N^+ &= [(a\delta - \alpha)(1 + a\delta) - \beta](1 + Na\delta) + [(a\delta - \alpha) - \beta(1 + a\delta)] + o(\delta) \\ &= 2(a - 1)\delta + o(\delta). \end{aligned}$$

182 To make $V_N^+(\lambda) = 0$, we conclude that $a = 1$. That is, $\lambda = \delta$ on the leading order. The
 183 positive eigenvalues for some small $\delta = \alpha + \beta$ are listed in Table 1 (all computed with
 184 $N = 40$). We observe that the dependence on the particular choice of α and β gets weaker
 185 as δ decreases. For the last three rows, we have $\delta N = 0.04$, and the maximal positive
 186 eigenvalues are very close to $\delta = 0.001$.

187 We remark that $\alpha + \beta = 0$ is equivalent to the long-wave limit property for a boundary
 188 condition in the form of (2.1a) or (2.1d). A minor violation of this condition may lead to a
 189 very small yet non-zero eigenvalue. In real applications, particularly when a more com-
 190 plex boundary condition is adopted, the long-wave limit property may likely be slightly
 191 violated. If the violation leads to a positive eigenvalue, the long-time instability occurs.
 192 This has been observed by some practitioners for absorbing boundary condition compu-
 193 tations. Because of the smallness of the eigenvalue, the unstable mode usually reaches an
 194 observable magnitude only after a long run, typically long after the main wave package
 195 reaches at the boundary and gets well absorbed. Furthermore, if δ is negative instead,
 196 the instability does not occur. As the boundary condition with $|\delta| \ll 1$ is viewed as a per-

Table 1: Maximal positive eigenvalue.

$\alpha + \beta$	α	β	$\max \lambda_+$
0.1	-1	1.1	0.0540
0.1	-0.9	1	0.0410
0.1	0	0.1	0.0909
0.01	-1	1.01	0.0085
0.01	-0.99	1	0.0086
0.01	0	0.01	0.0095
0.001	-1	1.001	0.00098
0.001	-0.999	1	0.00098
0.001	0	0.001	0.00095

197 perturbation from $\delta = 0$, instability presents only for a positive δ . The complexity makes the
 198 long time instability a hidden problem for most calculations.

199 In the multiscale computation community, the instability is usually regarded as the
 200 numerical error accumulation. As a matter of fact, for $\delta < 0$, numerical error also accumu-
 201 lates, yet it does not lead to indefinite growth of the total energy. Instead, the total energy
 202 is eventually damped out to the level of round-off error. By comparing with the case of
 203 $\delta > 0$, we show that this weak instability for the boundary condition better explains the
 204 phenomenon.

The long time instability occurs not only for the velocity boundary conditions. For
 instance, with a verlet algorithm to solve the Newton equations at a time step size $\Delta t =$
 $1/64$, a dynamic atomistic-continuum method takes the following boundary condition
 [6]:

$$u_0^{k+1} = \eta u_0^k - 0.074207u_1^k - 0.014903u_2^k - 0.95406u_0^{k-1} \\ + 0.074904u_1^{k-1} + 0.015621u_2^{k-1}, \quad (4.1)$$

$$u_{N+1}^{k+1} = \eta u_{N+1}^k - 0.074207u_N^k - 0.014903u_{N-1}^k - 0.95406u_{N+1}^{k-1} \\ + 0.074904u_N^{k-1} + 0.015621u_{N-1}^{k-1}. \quad (4.2)$$

205 Here $u_n^k = u_n(k\Delta t)$, and the coefficient η is suggested as 1.95264 in [6]. With this choice,
 206 it may be shown that the energy decays monotonically. However, if we take $\eta = 1.95265$
 207 instead, a slow exponential growth appears after a long run. In Fig. 5, we display the cal-
 208 culation for a 401-atom-chain with initial data shown in the second subplot. The waves
 209 are effectively absorbed at around $t = 200$ when they arrive at both ends. See the fourth
 210 subplot at $t = 300$. The unstable mode becomes evident at time around $t = 700$. In the
 211 last subplot for $t = 800$, the displacement profile is exactly the unstable eigen-mode. This
 212 unstable mode keeps growing later on, and dominates the lattice motion. The growth
 213 can be observed clearly from the energy in the first subplot. We remark that the latter
 214 choice of η violates the long wave limit property $R(0) = 0$. In the original design for the
 215 atomistic-continuum method, $R(0) = 0$ is taken as a constraint for the reflection mini-

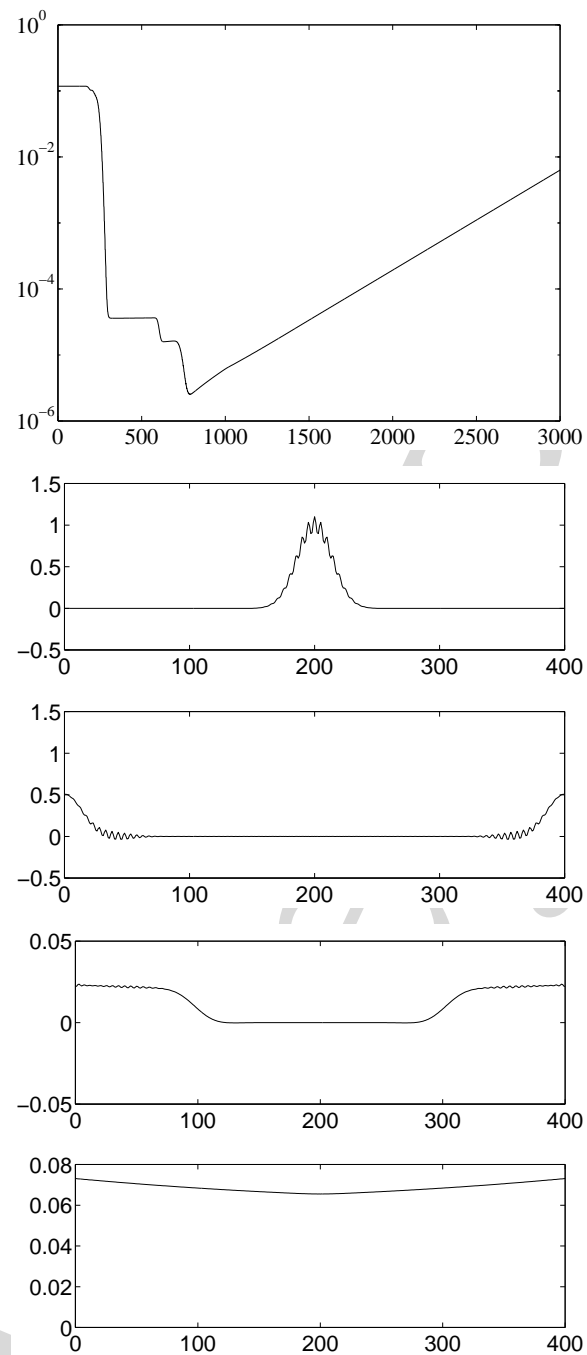


Figure 5: Long time instability in a dynamic atomistic-continuum calculation with a perturbed boundary condition. Subplots from top to bottom: evolution of the total energy (horizontal axis for time); displacements at $t=0$, $t=200$, $t=300$, and $t=800$.

216 mization problem. With the numerical example, we demonstrate the importance of this
217 constraint.

218 5 Conclusion

219 In this study, we check the validity of the reflection coefficient approach, which has been
220 widely adopted in the community of theoretical and computational physics. Through
221 careful explorations on a finite chain under a class of velocity boundary conditions, we
222 have revealed the deficiency of this approach. The cause for the deficiency lies in the
223 known fact that the Fourier modes are not the eigen-modes in general. We discover
224 that unstable surface modes exist with non-sinusoidal profiles, in a parameter range
225 where the reflection coefficient approach claims to be stable. Furthermore, we studied the
226 boundary condition which slightly violates the long-wave-limit property. A very small
227 yet positive eigenvalue may appear, leading to the long time instability, which have been
228 observed by some practitioners.

229 We would like to remark that this study mainly focuses on the unstable modes. Nu-
230 merical tests indicate that we do have stability away from the parameter region where the
231 unstable surface modes exist. Furthermore, the existence of such modes may be searched
232 from a low order polynomial, which greatly reduces the complexity of stability analysis.
233 The method we proposed may be extended to more general lattices.

234 The deficiency of the reflection coefficient approach requires revisits of the wave prop-
235 agations in physical sciences, as well as numerical algorithms. This may be particularly
236 critical at micro- or nano-scale. Absorbing boundary conditions for wave propagation
237 computations in an unbounded domain, or multi-scale computations with absorbing
238 boundary conditions are two important topics where the fidelity of the reflection coef-
239 ficient analysis needs better clarified. Moreover, it would be our future work to extend
240 the analysis to the stability in multiple dimensions, on which many important contribu-
241 tions have been made by Li *et al* [16], Liu's group [11, 19, 26] and many other researchers.

242 Acknowledgments

243 We are grateful to the anonymous referees for their stimulating discussions. This study
244 is supported in part by NSFC under contract number 10872004, National Basic Research
245 Program of China under contract number 2007CB814800, and the China Ministry of Ed-
246 ucation under contract numbers NCET-06-0011 and 200800010013.

247 A Semi-infinite chain

248 To better understand the deficiency of the reflection coefficient approach, we consider a
249 semi-infinite chain

$$\dot{u}_0 = \alpha u_0 + \beta u_1, \quad (\text{A.1a})$$

$$\dot{u}_n = v_n, \quad n = 1, \dots, N, \dots, \quad (\text{A.1b})$$

$$\dot{v}_n = u_{n-1} - 2u_n + u_{n+1}, \quad n = 1, \dots, N, \dots. \quad (\text{A.1c})$$

250 By a similar argument we find that $u_n(t) = \tilde{u}_n e^{\lambda t}$ with $\tilde{u}_n = Aq_+^n + Bq_-^n$. The boundary
251 condition reads

$$\lambda \tilde{u}_0 = \alpha \tilde{u}_0 + \beta \tilde{u}_1. \quad (\text{A.2})$$

252 To find the unstable modes, we seek for a real eigenvalue λ . Corresponding to such
253 an eigenvalue, we know from $q_+ > 1$ that $A=0$ for a motion with a finite total energy. The
254 boundary condition then gives

$$\lambda = \alpha + \beta q_-. \quad (\text{A.3})$$

255 This algebraic equation is equivalent to (3.10). It has a positive root λ for either $\alpha \leq$
256 $1, \beta > -\alpha$; or $\alpha > 1, -\alpha > \beta > -(\alpha + 2\sqrt{\alpha^2 + 3})/3[2\alpha^2 + 3 - 2\alpha\sqrt{\alpha^2 + 3}]$. The neutral stability
257 curve is depicted in Fig. 6. The eigen-mode has an exact form of $u_n(t) = q^n e^{\lambda t}$, which
258 exponentially decays in depth, and exponentially grows in time. Again, the reflection
259 coefficient approach can not account for the instability of the surface modes.

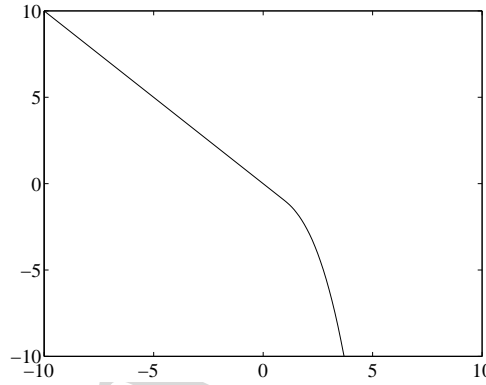


Figure 6: Neutral stability curve for a semi-infinite chain in (α, β) plane. Unstable surface modes exist for parameter above the curve.

260 B Stability analysis for general boundary conditions

We consider a class of more general boundary conditions.

$$\dot{u}_0 = \alpha u_0 + \sum_{j=1}^J \beta_j u_j, \quad (\text{B.1a})$$

$$\dot{u}_{N+1} = \alpha u_{N+1} + \sum_{j=1}^J \beta_j u_{N+1-j}. \quad (\text{B.1b})$$

261 The reflection coefficient is

$$R(k) = -\frac{\left(\alpha + \sum_{j=1}^J \beta_j \cos jk\right) + i\left(\sum_{j=1}^J \beta_j \sin jk - 2\sin(k/2)\right)}{\left(\alpha + \sum_{j=1}^J \beta_j \cos jk\right) - i\left(\sum_{j=1}^J \beta_j \sin jk + 2\sin(k/2)\right)}. \quad (\text{B.2})$$

We have $|R| < 1$ under the condition

$$\sum_{j=1}^J \beta_j \sin jk > 0.$$

262 With the previous $q_{\pm}(\lambda)$, we may find that an eigenvalue is a root to

$$W_N^{\pm}(\lambda) = \left[(\lambda - \alpha)q_+^{N+1} - \sum_{j=1}^J \beta_j q_+^{N+1-j} \right] \pm \left[\lambda - \alpha - \sum_{j=1}^J \beta_j q_+^j \right] = 0. \quad (\text{B.3})$$

As $\lambda \rightarrow +\infty$, we have $W_N^{\pm}(\lambda) \rightarrow +\infty$. At $\lambda = 0$, we find that

$$W_N^+(0) = -2\left(\alpha + \sum_{j=1}^J \beta_j\right), \quad W_N^-(0) = 0,$$

263 and

$$\frac{dW_N^-(0)}{d\lambda} = -\left[\alpha(N+1) - \sum_{j=1}^J \beta_j(N+1-2j)\right].$$

At $\lambda = \alpha$, we have

$$W_N^{\pm}(\alpha) = -\sum_{j=1}^J \beta_j (q_+^{N+1-j} \pm q_+^j).$$

Therefore, a positive eigenvalue λ_+ exists for $W_N^+(\lambda_+) = 0$ if $\alpha + \sum_{j=1}^J \beta_j > 0$. The eigenvalue $\lambda_+ > \alpha$ if both

$$\alpha > 0 \quad \text{and} \quad \sum_{j=1}^J \beta_j (q_+^{N+1-j} + q_+^j) > 0.$$

There also exists another positive eigenvalue $\lambda_- > 0$ for $W_N^-(\lambda_-) = 0$, if

$$\alpha - \sum_{j=1}^J \frac{\beta_j(N+1-2j)}{N+1} > 0.$$

The eigenvalue $\lambda_- > \alpha$ if both

$$\alpha > 0 \quad \text{and} \quad \sum_{j=1}^J \beta_j (q_+^{N+1-j} - q_+^j) > 0.$$

264 The eigenvector corresponding to an eigenvalue that is a root to $W_N^+(\lambda_+)$ is symmet-
 265 ric. Up to a factor, it is

$$\tilde{u}_n = \sum_{j=1}^J \beta_j \left(q_+^{N+1-n+j} - q_+^{N+1-n-j} + q_+^{n+j} - q_+^{n-j} \right).$$

266 The eigenvector corresponding to $W_N^-(\lambda_-)$ is antisymmetric. It may be taken as

$$\tilde{u}_n = \sum_{j=1}^J \beta_j \left(q_+^{N+1-n+j} - q_+^{N+1-n-j} - q_+^{n+j} + q_+^{n-j} \right).$$

267

268 References

- 269 [1] S.A. Adelman, and J.D. Doll, J. Chem. Phys. 61 4242 (1974).
 270 [2] R.E. Allen, G.R. Alldredge, and F.W. de Wette, Phys. Rev. B 4 1648 (1971).
 271 [3] X. Antoine, A. Arnold, C. Besse, M. Ehrhardt, and A. Schädle, Commun. Comput. Phys. 4(4)
 272 729 (2008).
 273 [4] L. Brekhovskikh, and V. Goncharov, Mechanics of Continua and Wave Dynamics, Springer,
 274 Berlin, (1985) p. 65-69.
 275 [5] W. Cai, M. de Koning, V.V. Bulayov, and S. Yip, Phys. Rev. Lett. 85 3213 (2000).
 276 [6] W. E, and Z.Y. Huang, J. Comput. Phys. 182 234 (2002).
 277 [7] B. Engquist, and A. Majda, Math. Computation 31 629 (1977).
 278 [8] T. Ha-Duong, and P. Joly, Math. Computation 62 539 (1994).
 279 [9] L. Halpern, Math. Computation 38 415 (1982).
 280 [10] E. Herrin, and T. Goforth, Bull. Seismological Soc. Amer. 67 1259 (1977).
 281 [11] E. G. Karpov, G. J. Wagner, and W. K. Liu Int. J. Numer. Methods Engrg. 62 1250 (2005).
 282 [12] R.L. Higdon, SIAM J. Numer. Anal. 31 64 (1994).
 283 [13] J.B. Keller, and D. Givoli, J. Comput. Phys. 82 172 (1989).
 284 [14] H. O. Kreiss, Comm. Pure Appl. Math. 23 277 (1970).
 285 [15] X. Li, J. Comput. Appl. Math. 231 493 (2009).
 286 [16] X. Li, and W. E, Commun. Comput. Phys. 1 136 (2006).
 287 [17] Z.P. Liao, Introduction to Wave Motion Theories in Engineering (2nd ed.), Science Press,
 288 Beijing, (2002) p. 136-189 (in Chinese).
 289 [18] A.B. Manenkov, IEE Proc. J. Optoelectronics 139 101 (1992).
 290 [19] H. Park, E. G. Karpov, P. Klein, and W. K. Liu, J. Comput. Phys. 207 588 (2005).
 291 [20] D. Qian, G.J. Wagner, and W.K. Liu, Comput. Methods Appl. Mech. Engrg. 193 1603 (2004).
 292 [21] L. Rayleigh, Proc. London Math. Soc. s1-17 4 (1885).
 293 [22] S.Y. Ren, Phys. Rev. B 64 035322 (2001).
 294 [23] S.Q. Tang, T.Y. Hou, and W.K. Liu, J. Comput. Phys. 213 85 (2006).
 295 [24] S.Q. Tang, J. Comput. Phys. 227 4038 (2008).
 296 [25] A. To, and S. Li, Phys. Rev. B 72 035414 (2005).
 297 [26] G. J. Wagner, E. G. Karpov, and W. K. Liu, Comput. Methods Appl. Mech. Engrg. 193 1579
 298 (2004).
 299 [27] D. Yang, S. Wang, Z. Zhang, and J. Teng, Bull. Seism. Soc. Am. 93 2389 (2003).